Microstructure and texture in cryomilled and spark plasma sintered Ti Grade 2

Jiří Kozlík[1*], Josef Stráský[1], Petr Harcuba[1], Tomáš Chráska[2], Miloš Janeček[1]

[1] Department of Physics of Materials, Charles University, Prague, Czechia

[2] Institute of Plasma Physics, Czech Academy of Science, Prague, Czechia

* E-mail: jiri.kozlik@mff.cuni.cz

Abstract

Titanium (Grade 2) was processed by cryogenic milling and subsequently sintered by spark plasma sintering (SPS) method with the aim of creating and preserving the ultra-fine grained (UFG, < 1 μm) microstructure. Microstructural investigation was performed after both cryogenic milling and spark plasma sintering. An advanced technique of transmission Kikuchi diffraction (TKD) was used to characterize the individual milled powder particles.

Investigations of milled powders showed significant grain refinement down to 50 nm after milling in liquid argon with tungsten carbide balls. We assume that this is the equilibrium grain size resulting from the balance of deformation, recovery and dynamic recrystallization. A texture, resembling the rolling texture in Ti, was also found in the milled particles, which can be explained by the nature of deformation during milling.

UFG microstructure was not maintained after sintering, with the mean grain size of 2.6 μm. Although the grains are completely recrystallized, a texture, similar to the powder texture, was also found in these samples as a result of packing of the powder particles and the nature of the recrystallization process (continuous static recrystallization).

1. Introduction

Titanium, as an important metal with a good corrosion resistance, biocompatibility and high specific strength [1], can benefit from the powder metallurgy processing routes. Its machining is difficult because of the low thermal conductivity and high toughness and its casting faces issues with contamination by oxygen and nitrogen. The powder metallurgy then seems to be a viable route towards near-net shape processing [2].

The methods of thermomechanical processing of bulk materials are well established, but there are methods for processing of powders as well. Ball milling is a powder metallurgy process which causes deformation and potential fragmentation of powder particles. Grain refinement might be caused by ball milling due to repetitive plastic deformation [3]. The ultra-fine grained microstructure, if preserved in the bulk material, can contribute to the strength enhancement [4,5] via Hall-Petch (grain boundary) strengthening.

Naturally, there are other processes taking place during milling, which act against the microstructural refinement – recovery and dynamic recrystallization [3]. Because both are thermally driven, they can be suppressed by lowering the processing temperature to liquid nitrogen/argon temperatures. This process is then called cryogenic milling and numerous materials were already processed by this method, for example Inconel [6], Al [7,8] and Mg [9].

Cryogenic milling of titanium is feasible only in liquid argon (LAr), since liquid nitrogen (LN) heavily contaminates the powder [10–12]. The process control agent (e.g. stearic acid) must be used to prevent cold-welding of particles [11]. Heavy WC balls are more efficient in terms of reducing particle size – the similar degree of particle fragmentation is achieved after less than half of the milling time needed by stainless steel balls [11,13]. Titanium remains ductile even at cryogenic temperatures under LAr environment and the particles after milling have flaky / disc-like shape with their diameter ranging approximately from 50 to 100 μm and with thickness of 10 μm at most [11]. The investigation of microstructure could show whether the higher energy of impact caused by utilization of WC balls result also in more severe deformation and grain refinement.

The detailed investigations of the powder particle microstructure was made possible by a transmission electron backscatter diffraction (tEBSD) / transmission Kikuchi diffraction (TKD) method, significantly enhancing the spatial resolution of the conventional EBSD to the level of several nanometers [14,15].

Spark plasma sintering (SPS) method is nowadays a popular sintering technique, mainly because of its short processing times (in order of minutes or tens of minutes). This can be beneficial for the sintering of ultra-fine grained materials due to overcoming problems with the excessive grain growth. Nevertheless, it was found that even short sintering times are used, ultra-fine grained microstructure is not preserved in the unalloyed titanium sintered to achieve the full density [10,13].

It was recently found that significant texture evolves during milling and that this texture can be preserved even after recrystallization during sintering [13].

The main aim of this paper is to characterize the microstructure and texture of an individual powder particle processed by milling with WC balls and to compare it with the previous results obtained with stainless steel balls. The comparison of the powder and bulk material microstructure is also performed to show its evolution during sintering.

2. Experimental methods

Commercially pure Ti powder (Grade 2), supplied by TLS Technik, GmbH, Germany, was used as a starting material. The content of contaminants was 0.006 wt% of C, 0.08 wt% of Fe, 0.001 wt% of H, 0.004 wt% of N and 0.14 wt% of O. Powder was prepared by gas atomization method and consisted spherical particles of (20–60) μm in diameter.

The cryogenic milling was conducted in the Union Process 01-HD attritor in a stainless steel tank with the volume of 1400 cm^3. Tungsten carbide (WC) balls with the density of 15.6 g/cm^3 were used as a heavy and hard milling medium with ball-to-powder ratio (BPR) of 32:1. Stearic acid (SA) was used as a process control agent to avoid cold-welding and to enhance the process yield. The milling was performed in a bath of liquid argon (LAr) at (-186 ± 5) °C for 3.25 h (the milling time was restricted due to a limited available amount of LAr) at the speed of 650 rpm. The powder was cleaned from the remnants of SA by repeated washing in ethanol and filtration.

The sintering was done in the SPS 10-4 furnace (Thermal Technology LLC) in a graphite die. The samples of 20 mm in diameter and approx. 6 mm in height were produced. Fast sintering program was applied, utilizing the benefits provided by the SPS. The samples were heated from room temperature up to 750 °C in 1 min and then to the desired sintering temperature of 800 °C in 30 s (to avoid temperature overshooting during heating). The isothermal sintering was then performed for 3 min, followed by a free cooling with an uncontrolled cooling rate; approximate cooling rate is 200 °C/min at the beginning of cooling and then decreases exponentially. The uniaxial pressure of 80 MPa was used.

The characterization was performed using a Zeiss Auriga Compact FIB-SEM scanning electron microscope, equipped with EDS and EBSD detectors and a 20° holder for tEBSD samples. A lamella was prepared by focused ion beam (FIB) milling from an individual powder particle such that the observation plane is perpendicular to the flat surface of the particle. The lamella with the two thinned ‘windows’ used for tEBSD mapping is shown in the Fig. 1.

The amount of oxygen, hydrogen and nitrogen in the material was determined by the carrier-gas hot extraction (CGHE) method.

3. Results and discussion

The milled powder consists of flat /disc-like particles, as shown in the Fig. 1a. The contamination of the powder after milling and cleaning was measured by CGHE: 0.59 wt% of O, 0.08 wt% of N and 0.03 wt% of H.

The microstructure was investigated by tEBSD in the two ‘windows’ transparent for electron beam, one near the particle’s center and the second one near its edge, as shown in the Fig. 1b and 1c. The mapping was done with the step size of 13 nm (this was a compromise between the spatial resolution and the drift during scanning). The resulting maps are shown in the Fig. 2. The drift during data acquisition was manually corrected after the measurement.

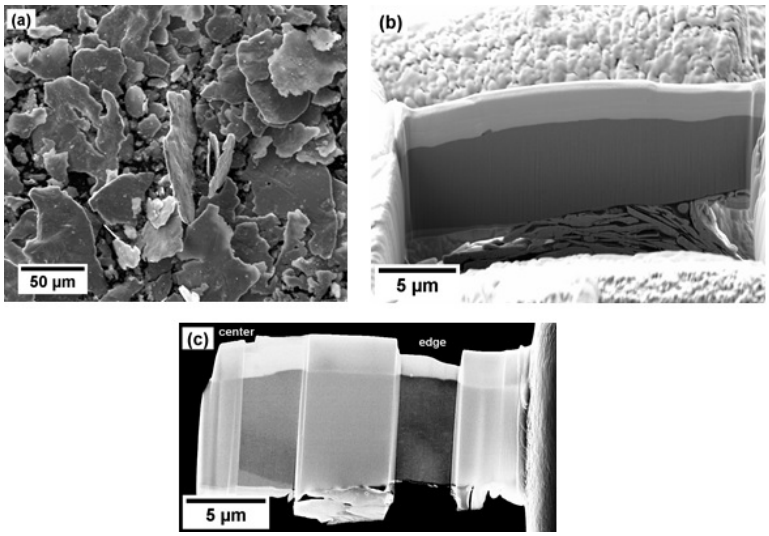

Fig 1: (a) An SEM micrograph of the milled powder morphology. (b) and (c) show the lamella cut for the tEBSD investigations. (b) A perpendicular cut across the powder particle (its edge is to the right). (c) The final polished lamella with the two observation 'windows' used for tEBSD mapping.

The maps show bimodal grain morphology in both regions, more pronounced in the edge region (Fig. 2b). There is a majority of small, equiaxed grains with the size in the range of 50 to 80 nm, but there is also a considerable number of larger grains elongated in the horizontal direction and a broad distribution of grain sizes. These grains also exhibit cellular subgrain structure, which can be seen especially in the large grains in Fig 2b.

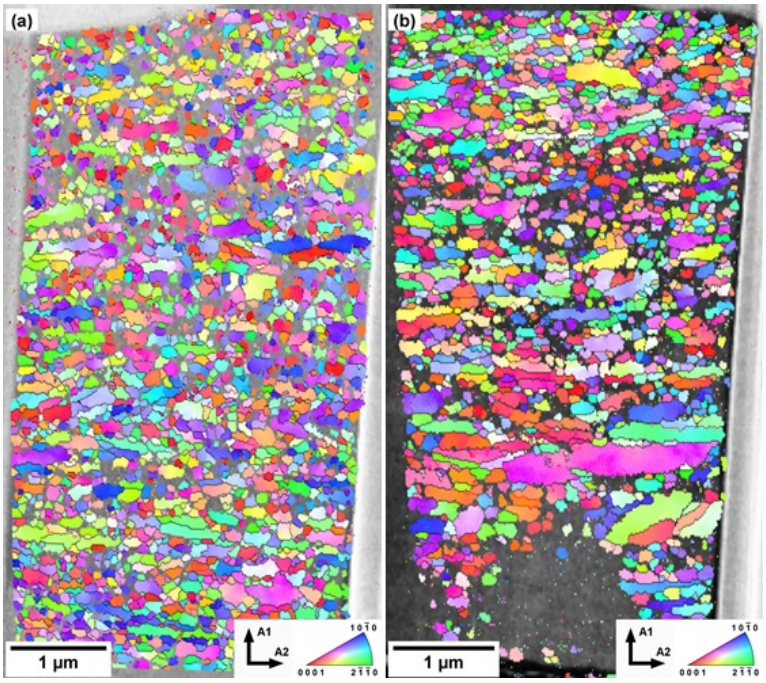

Fig 2: IFP maps of tEBSD investigations of the central (a) and edge (b) area of the powder particle (cf. Fig 1b), the color is drawn for the A1-A2 plane (i.e. the lamella plane) The IPF maps are overlaid over the SEM image of the lamella. High-angle grain boundaries (HAGB, > 15°) are marked with black lines, low-angle grain boundaries (LAGB, 5–15°) are marked with red lines.

As can be concluded from Fig. 2, the microstructure within the sample is nonhomogeneous. The central region (Fig 2a) clearly shows larger amount of equiaxed grains and more homogeneity within the window, although the horizontally elongated grains are also present. On the other hand, the edge region contains some comparatively very large grains (> 1 µm) in the bottom of the map and smaller and more equiaxed grains at its top. It can be concluded from these observations that the deformation during the milling is not homogeneous within the particle, resulting in the non-homogeneous microstructure.

The microstructure observations are consistent with the earlier results reporting similar bimodal grain morphology [11,13]. Ertorer et al. [10] reported smaller grains of ~20 nm after milling for 8 h in LAr, but the amount nitrogen (0.59 wt%) was significantly higher than in the material used in this study (0.08 wt%) and which is known to impede the grain boundary movement and suppress recovery and recrystallization. On the other hand, increased nitrogen content also causes material embrittlement and therefore cannot be efficiently utilized for microstructural refinement. The presence of larger grains is also consistent with the general mechanism of grain refinement during severe plastic deformation [16]: the starting grains are deformed, a dislocation network and a subgrain structure is formed and from these subgrains, small equiaxed grains are finally formed. During intensive plastic deformation, grain size cannot be reduced below a certain limit due to recovery and static recrystallization [17]. Such limit was reached in the case of the small equiaxed grains, reaching the same grain size as for powders prepared under different milling conditions [11,13]. It should be noted that this minimum value is dependent on the material composition (e.g. on the impurities content) and also on the processing temperature, because both parameters influence kinetics of recovery and dynamic recrystallization.

The large elongated grains with subgrain structure (LAGBs are marked by red lines in Fig. 2) can be viewed as not fully refined yet and the prolonged milling would lead to the creation of the small equiaxed grains as well.

The microstructure of a fully sintered material (with relative density > 99.5 %) is shown in the Fig 3. The grains were completely recrystallized and the mean grain size was 2.6 µm. This is lower than in the previous study [13], which is the result of grain boundary pinning by oxygen and by fragments of WC balls [18].

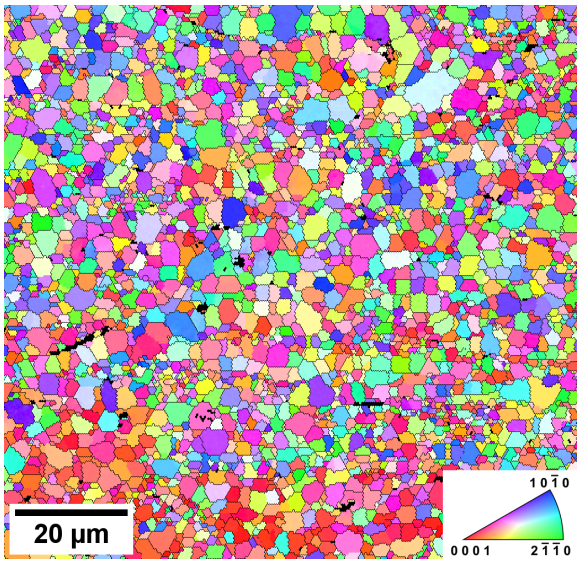

Fig 3: The IPF map of a sample sintered at 800 °C for 3 min showing completely recrystallized microstructure. HAGBs (> 15°) are marked with black lines), the color is drawn for the A1-A2 plane.

The texture was investigated in both observed regions ('windows') in the milled powder and in the sintered sample. The resulting pole figures are shown in Fig. 5. The most prominent feature is the arrangement of the (0001) poles in a conical fashion around the A1 axis, with the apex half-angle of approx. 20–40° (can be best seen in the Fig. 4c, although similar arrangement is present in all pole figures). This texture is similar to the rolling texture in Ti, although the rolling texture exhibits only two (0001) poles. The observed texture is created as a result of repeated impacts of milling balls, causing deformation with compression and shear component similar to deformation during rolling. However, rolling direction and transverse direction are not defined in the case of milling (each impact comes from an arbitrary direction) and the only direction remaining constant is the normal to the surface of the powder particle (corresponding to the normal direction during rolling and to the A1 axis in the Fig. 4). After milling, the flat powder particles are preferentially arranged in the horizontal direction in the die during sintering. In such case, the texture of the sintered material is created by many textured powder particles, which are not arranged randomly, but have a common normal to the flat particle surface (= A1 direction).

Such kind of a texture was already reported for the powder cryomilled using stainless steel balls, along with its transfer to the sintered material [13]. The transfer of a texture is enabled by so-called *continuous static recrystallization* mechanism [19], which does not include a nucleation of new, randomly oriented grains, but rather a rapid growth of some of the preexistent ones. This process then results in preserving the texture of a starting material, which was reported also for AZ31 magnesium alloy [20].

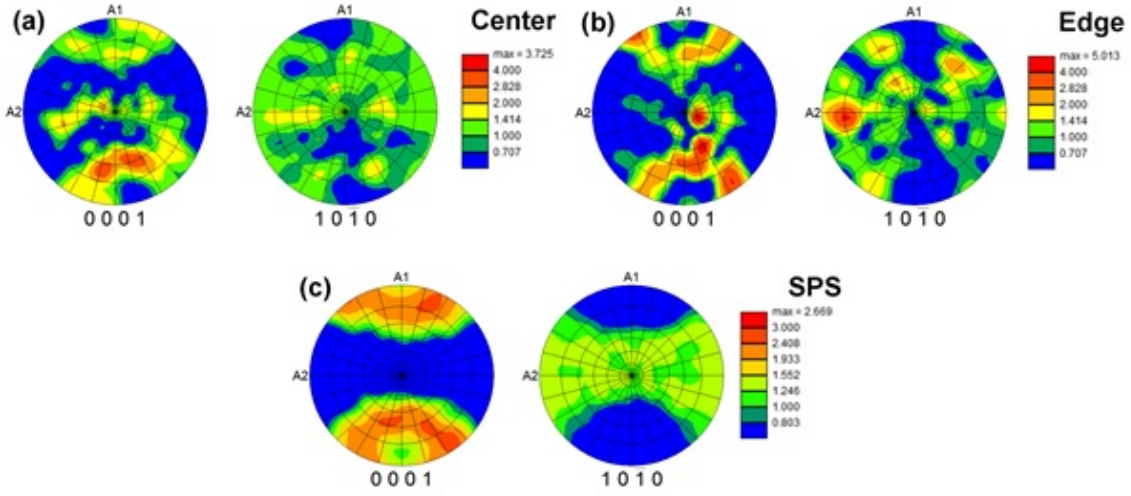

Fig 4: Pole figures of both milled and sintered material. Note that the texture maxima values are not directly comparable, since they have the meaning of a "texture density" (and therefore comparatively lower value is found in the (c) subfigure with larger non-discrete maxima).

A texture developed by the same mechanism was also reported for cryomilled and sintered magnesium [9]. Magnesium after rolling normally exhibits a basal texture with one (0001) pole pointing towards the normal direction. Powder particles were similarly flat after milling, which resulted in their preferential arrangement, and via the same mechanism, the texture of the

individual particles was transferred to the bulk material, resulting in a basal texture. Note that although both magnesium and titanium are hcp metals, primary slip systems are different due to different c/a ratio.

4. Conclusions

The microstructure of Ti powder which was cryogenically milled with the use of tungsten carbide balls (investigated using tEBSD) and its microstructure after spark plasma sintering (investigated by EBSD) is presented. The main results can be summarized as follows:

- The grain morphology is bimodal, with smaller equiaxed and larger elongated grains.
- The equilibrium grain size of 50–80 nm was achieved in multiple region of the powder particle. Utilization of tungsten carbide balls does not lead to further grain refinement when compared to milling using stainless steel balls. This can be attributed to achieving minimum attainable grain size which depends mainly on material and processing temperature.
- The milled material is textured and this texture is preserved during sintering due to continuous static recrystallization.

Acknowledgements

This work was financially supported by the Czech Science Foundation under project No. 19-11275S. The partial financial support provided by ERDF under the project No. CZ.02.1.01/0.0/0.0/15 003/0000485 is also gratefully acknowledged.

References

[1] G. Lütjering, J.C. Williams, Titanium, Springer Berlin Heidelberg, Berlin, Heidelberg, 2007.

[2] M. Qian, F.H. Froes, eds., Titanium Powder Metallurgy, Elsevier, Boston, 2015.

[3] C. Suryanarayana, Prog. Mater. Sci. 46 (2001) 1–184.

[4] E.O. Hall, Proc. Phys. Soc. Sect. B 64 (1951) 747–53.

[5] N.J. Petch, J. Iron Steel Inst. 174 (1953) 25–28.

[6] J. He, E.J. Lavernia, J. Mater. Res. 16 (2001) 2724–2732.

[7] H.-B. Chen, K. Tao, B. Yang, J.-S. Zhang, Trans. Nonferrous Met. Soc. China 19 (2009) 1110–1115.

[8] F. Zhou, D. Witkin, S.R. Nutt, E.J. Lavernia, Mater. Sci. Eng. A 375–377 (2004) 917–921.

[9] X. Wang, L. Jiang, D. Zhang, I.J. Beyerlein, S. Mahajan, T.J. Rupert, E.J. Lavernia, J.M. Schoenung, Acta Mater. 146 (2018) 12–24.

[10] O. Ertorer, A. Zúñiga, T. Topping, W. Moss, E.J. Lavernia, Metall. Mater. Trans. A 40 (2008) 91–103.

[11] J. Kozlík, J. Stráský, P. Harcuba, I. Ibragimov, T. Chráska, M. Janeček, Metals 8 (2018) 31.

[12] F. Sun, P. Rojas, A. Zúñiga, E.J. Lavernia, Mater. Sci. Eng. A 430 (2006) 90–97.

[13] J. Kozlík, P. Harcuba, J. Stráský, H. Becker, J. Šmilauerová, M. Janeček, Mater. Charact. 151 (2019) 1–5.

[14] R.R. Keller, R.H. Geiss, J. Microsc. 245 (2012) 245–251.

[15] T. Tokarski, G. Cios, A. Kula, P. Bała, Mater. Charact. 121 (2016) 231–236.

[16] T.G. Langdon, Acta Mater. 61 (2013) 7035–7059.

[17] F.A. Mohamed, Acta Mater. 51 (2003) 4107–4119.

[18] J. Kozlík, P. Harcuba, J. Stráský, T. Chráska, M. Janeček, in: Met. 2018 - 27th Anniv. Int. Conf. Metall. Mater. Conf. Proc., 2018, pp. 1298–1303.

[19] R.D. Doherty, D.A. Hughes, F.J. Humphreys, J.J. Jonas, D.J. Jensen, M.E. Kassner, W.E. King, T.R. McNelley, H.J. McQueen, A.D. Rollett, Mater. Sci. Eng. A 238 (1997) 219–274.

[20] X. Yang, H. Miura, T. Sakai, Mater. Trans. 46 (2005) 2981–2987.